Competing mechanisms in the atomic diffusion of a MgO admolecule on the MgO(001) surface

2009 J. Phys.: Condens. Matter 21 315004

(http://iopscience.iop.org/0953-8984/21/31/315004)

IOP Publishing Journal of Physics: Condensed Matter

J. Phys.: Condens. Matter **21** (2009) 315004 (7pp) doi:10.1088/0953-8984/21/31/315004

Competing mechanisms in the atomic diffusion of a MgO admolecule on the MgO(001) surface

Grégory Geneste[1,2], **Marc Hayoun**[3], **Fabio Finocchi**[4] **and Joseph Morillo**[2]

[1] Laboratoire Structures, Propriétés et Modélisation des Solides, UMR CNRS 8580, Ecole Centrale Paris, Grande Voie des Vignes, 92295 Châtenay-Malabry Cedex, France
[2] Centre d'Élaboration de Matériaux et d'Études Structurales, UPR CNRS 8011, 29 rue Jeanne Marvig, 31055 Toulouse Cedex 4, France
[3] Laboratoire des Solides Irradiés, Ecole Polytechnique, CEA-DSM, CNRS, 91128 Palaiseau, France
[4] Institut des Nanosciences de Paris, UMR CNRS 7588 and Universités Paris 6-Paris 7, Campus de Boucicaut, 140 rue de Lourmel, 75015 Paris, France

E-mail: marc.hayoun@polytechnique.edu

Received 19 February 2009, in final form 5 June 2009
Published 7 July 2009
Online at stacks.iop.org/JPhysCM/21/315004

Abstract

The diffusion mechanism of a MgO admolecule on a flat MgO(001) surface has been investigated by equilibrium molecular dynamics simulation. Care has been taken in the choice of the phenomenological interionic potential used. Four distinct mechanisms have been found and the corresponding dynamical barriers determined at high temperature. Some static barriers have also been computed for comparison and all intermediate configurations have been obtained with the same phenomenological potential and also by the DFT-GGA approach. The hopping mechanisms involving the Mg adatom, although dominant, must be combined with the infrequent mechanisms involving displacements of O adatoms in order to provide the mass transport on the surface, which is crucial for crystal growth both in the nucleation and step-flow regimes.

(Some figures in this article are in colour only in the electronic version)

1. Introduction

The surface diffusion of adatoms and admolecules is a fundamental phenomenon of crystal growth. Surface diffusion of metal adatoms on metallic surfaces [1] or admolecules on semiconductor surfaces [2] is now fairly well understood due to a combination of extensive atomic scale experiments and numerical simulations, either from phenomenological potentials or *ab initio* methods.

However, we have much less knowledge concerning oxides. Yet these materials are of primary interest as thin/ultrathin films in various applications (sensors, catalysts, electronic devices, spin valves [3]), and their growth needs to be controlled with ever-increasing atomic scale accuracy.

A characteristic of such materials is the existence on the surface, during growth, of various chemical species in various oxidation states. We focus in this work on the emblematic case of MgO(001), a system on which the different species involved in the growth have already been identified (neutral Mg adatom, neutral O adatom, peroxide ion O_2^{2-}, ionic MgO molecule) [4–10]. In particular, we have explained how the atomic species (Mg and O adatoms) adsorb, diffuse [9] and stick together to form the diatomic MgO molecule through an oxoreduction chemical reaction. In recent theoretical papers, we reported precisely how such an entity forms during growth [10], and pointed out its fundamental role in the oxide growth process. Indeed, the MgO admolecule has the largest diffusion length and thus contributes crucially to matter transport on the terraces through surface diffusion.

The surface diffusion of this fundamental entity on the MgO(001) surface has been studied by various methods (*ab initio* calculations based on density-functional theory and

molecular dynamics simulations with empirical potentials), and several diffusion processes have been evidenced. Using *ab initio* methods, we have suggested the possibility of rotation of one ion around another and calculated the corresponding energy barriers within constrained optimization [5]. These values were confirmed later by Henkelman *et al* [11], who showed that the intermediate state was in fact a local minimum for all the processes considered. Interestingly, we have also evidenced, from molecular dynamics (MD) simulations, the existence of an original exchange mechanism, never reported to our knowledge for oxide materials, in which the molecular Mg cation exchanges with the surface Mg cation beneath the adsorbed oxygen ion [7, 8]. This mechanism was later confirmed by Harris *et al* [12] through MD, and thoroughly investigated by Henkelman *et al* [11] using static calculations.

However, a systematic dynamical and quantitative investigation of the diffusion mechanisms of this admolecule, giving access to the dynamical energy barriers, is still lacking. In the present work we investigated the surface diffusion of an MgO admolecule on the MgO(001) surface within MD, and evidenced four diffusion mechanisms referred to hereafter as Mg rotation, O rotation, Mg exchange and molecular jump. We performed an extensive statistical study of the jumps at different temperatures and deduced the dynamical energy barriers for each mechanism using Arrhenius plots. These results are obtained without any explicit approximation on the migration barriers and their crossing except for the interatomic potentials. They take into account: (i) the possible collective phenomena missing at $T = 0$ K; (ii) the possible barrier recrossing excluded within the transition state theory (transmission coefficient equal to 1); (iii) the anharmonic effects; in addition (iv) no hypothesis is made on the reaction path.

We also performed static calculations both within an *ab initio* approach and a phenomenological modelling, and considered the MgO admolecule in various configurations. Its stable position, as well as the intermediate configurations corresponding to Mg and O rotation, have been precisely described in [5]. In the present work we complete the energy landscape of the MgO admolecule with the intermediate states corresponding to the two other diffusion processes that will be extensively described hereafter.

2. Methods

2.1. Ab initio approach

We performed our *ab initio* computations in the framework of the density-functional theory (DFT) [13] within the ABINIT code [14]. We used the GGA-PBE functional [15] to model the exchange and correlation energy. Pseudopotentials of the Troullier–Martins type were used to account for the effects of core electrons (1s, 2s and 2p for Mg, 1s for O). The periodic parts of the Kohn–Sham wavefunctions were expanded in a plane-wave basis set with a cutoff of 28 Ha and periodic boundary conditions applied to the simulation cell. Atomic configurations were relaxed to the equilibrium within a damped molecular dynamics procedure, until the maximal forces were less than 0.05 eV Å^{-1} on unconstrained atoms.

A precise description of the fully relaxed MgO(001) surface can be attained using four-layer slabs separated by a vacuum thickness equivalent to four MgO layers [5], the atoms of the bottom surface being fixed in their bulk positions. The lateral size of the cell is two MgO bulk lattice parameters ($a_0 = 8.096$ Bohrs) which corresponds to a $2\sqrt{2} \times 2\sqrt{2}$ cell in terms of the primitive two-dimensional cell of the ideal MgO(001) surface. The Mg and O bulk (± 1.76), surface (± 1.72) and admolecule (± 1.52) topological charges, that were previously calculated [9, 7] by the Bader method [16], are rather close together.

The intermediate states observed during the diffusion of the MgO molecule correspond to local minima of the energy surface [11]. They are obtained from a geometric optimization, starting from a configuration in which the two ions of the molecule are placed in intermediate positions. These configurations are relaxed until the Cartesian components of the atomic forces are all below 0.05 eV Å^{-1}.

The *ab initio* approach, successfully compared to the existing experimental data [5, 6], also provides physical quantities which cannot be experimentally reached. The *ab initio* data are thus used in the present paper as reference values.

2.2. Phenomenological potentials

One of the analytical expressions of the rigid ion model (RIM) we used is given by relation (1):

$$V(r_{ij}) = q_i q_j / r_{ij} + A_{\alpha\beta} \exp(-r_{ij}/\rho_{\alpha\beta}) - (C_{\alpha\beta}/r_{ij}^6) \quad (1)$$

i and j are the labels of the ions of an interacting pair and each ion may have the α or β type ($\alpha, \beta = \text{Mg, O}$). The *ab initio* results [9, 7] have shown that the charges, q_i, vary little among the bulk, the surface and the admolecule. Constant charges for the Coulombic contributions are thus adopted. As usual, the Ewald method [17] has been used to calculate the Coulomb terms. We have selected four model potentials previously derived [18–21], referred to hereafter as Kubo, Shen, Okada and Matsui, respectively. Their parameters are reported in table 1. The main short-range contribution is the repulsive interaction between Mg and O which is necessary to counterbalance their electrostatic attraction. The contribution of the attractive O–O interaction is considered as relatively important due to the rather large oxygen ion size. The potential models may also include attractive and repulsive contributions for the other interactions. The short-range Mg–Mg contribution is small in magnitude; it is accounted for only by one of the model potentials [20].

2.3. Molecular dynamics

The analysis of the jump mechanisms responsible for the diffusion of the MgO admolecules on the (001) surface has been carried out on equilibrium atomic trajectories generated by MD. This study has required long trajectories up to 2 ns in the temperature range of 700–1100 K. The simulations were performed in the microcanonical ensemble with the rigid ion potentials described in section 2.2. The simulated system

Table 1. Potential parameters of the rigid ion model, corresponding bond lengths and energies of the free molecule. The formation enthalpies, ΔH_f, of various configurations including adsorbed clusters of n molecules can be compared to the DFT-GGA values. All quantities refer to $T = 0$ K.

	Kubo	Matsui	Okada	Shen	GGA
$\|q_{Mg}\| = \|q_O\|$	1.2	1.4	1.56	2.0	1.76
A_{Mg-Mg} (eV)	3943.8	1310 148	97 411	0	
A_{Mg-O} (eV)	63 619	9898	2498.9	1152	
A_{O-O} (eV)	872 184	2147	566.87	22 760	
ρ_{Mg-Mg} (Å)	0.160	0.104	0.150		
ρ_{Mg-O} (Å)	0.165	0.202	0.247	0.3065	
ρ_{O-O} (Å)	0.170	0.300	0.344	0.149	
C_{Mg-Mg} (eV Å^6)	0	0	0.390 25	0	
C_{Mg-O} (eV Å^6)	0	0	2.8625	0	
C_{O-O} (eV Å^6)	0	30.236	20.997	28.960	
Free MgO bond length (Å)	1.82	1.73	1.63	1.54	1.75
Free MgO bond energy (eV/MgO)	10.36	14.42	18.25	29.82	
Lattice parameter (Å)	4.191	4.201	4.192	4.222	4.28
Cohesive energy[a] (eV/MgO)	5.60	6.88	7.65	10.97	6.97
Surface ΔH_f (eV/MgO)	0.40	0.48	0.49	0.69	0.50
Step ΔH_f (eV/MgO)	0.66	0.72	0.72	1.00	0.88
Adsorption enthalpy (eV/MgO)	2.04	2.84	3.40	5.10	2.48
$\Delta H_f(n = 2)$	1.68	1.99	2.13	2.92	2.15
$\Delta H_f(n = 3)$	2.09	2.46	2.63	3.66	2.68
$\Delta H_f(n = 4)$	2.31	2.71	2.90	4.03	2.97
$\Delta H_f(n = 6)$	2.60	3.02	3.21	4.45	3.29
$\Delta H_f(n = 8)$	2.78	3.22	3.42	4.74	3.52

[a] With respect to free molecules.

contains at least 1728 ions. Periodic boundary conditions have been employed in the two directions parallel to the surface and the time step is equal to 2×10^{-15} s. Free boundary conditions are used in the direction perpendicular to the surface, thus creating a couple of parallel free surfaces separated by 23.1 Å (the system is 12 layers thick). One admolecule is added on each free surface, which improves the statistics of the diffusion processes. The values of the equilibrium bulk lattice parameter have been determined for each temperature; they yield a pressure close to zero.

2.4. Trajectory analysis

We have developed a code to analyse the migration of the admolecules from the MD trajectories. We have used the regular lattice sites of the atoms of the surface plane in order to localize the adatoms during their motion. An atomic site is defined by considering a circular surface centred on a regular lattice site. The value of the disc radius is chosen so that a diffusing atom leaving a regular site is discriminated from a vibrating atom with a large magnitude. In order to analyse the migration of the adatoms, we first performed 3D animations of atomic trajectories. This qualitative analysis leads to the identification of four atomic jumps drawn in figure 1. Then, criteria allowing the detection of these jumps were defined and introduced in the code in order to perform an automatic quantitative analysis: jump frequencies, times of flight, etc. The jump frequency of a given mechanism is defined as the number of occurrences of the repeating event per unit time. Five temperatures were investigated between 700 and 1100 K and the total number of jumps of the two admolecules ranged from 300 to 1150, respectively. Arrhenius plots were built from the jump frequencies of each mechanism and used to determine the activation energies associated with each mechanism.

3. Results and discussion

3.1. Choice of the phenomenological potential

In order to determine which of the four potentials of table 1 is adapted to our study, we decided to check their ability to reproduce the *ab initio* results [6].

The bond length of the isolated MgO and its bond energy as calculated with the various models are listed in table 1 and compared. The MgO bond of the Kubo potential can be too easily broken, whereas that of the Shen potential is too strong. The two other potentials provide acceptable results. The Matsui potential reproduces successfully the GGA value of the bond length.

The lattice constant of the MgO crystal is not a relevant parameter to discriminate the models because: (i) all values are very close to each other (indeed, they result from the fitting of the same experimental data); and (ii) the GGA approach systematically overestimates it. As far as the cohesive energy is concerned, the Matsui potential provides the value which is closer to the GGA one.

Another important quantity for this study is the surface formation enthalpy given in table 1. The surface energies calculated with the Okada and Matsui potentials agree very well with the GGA result. The value of the step formation

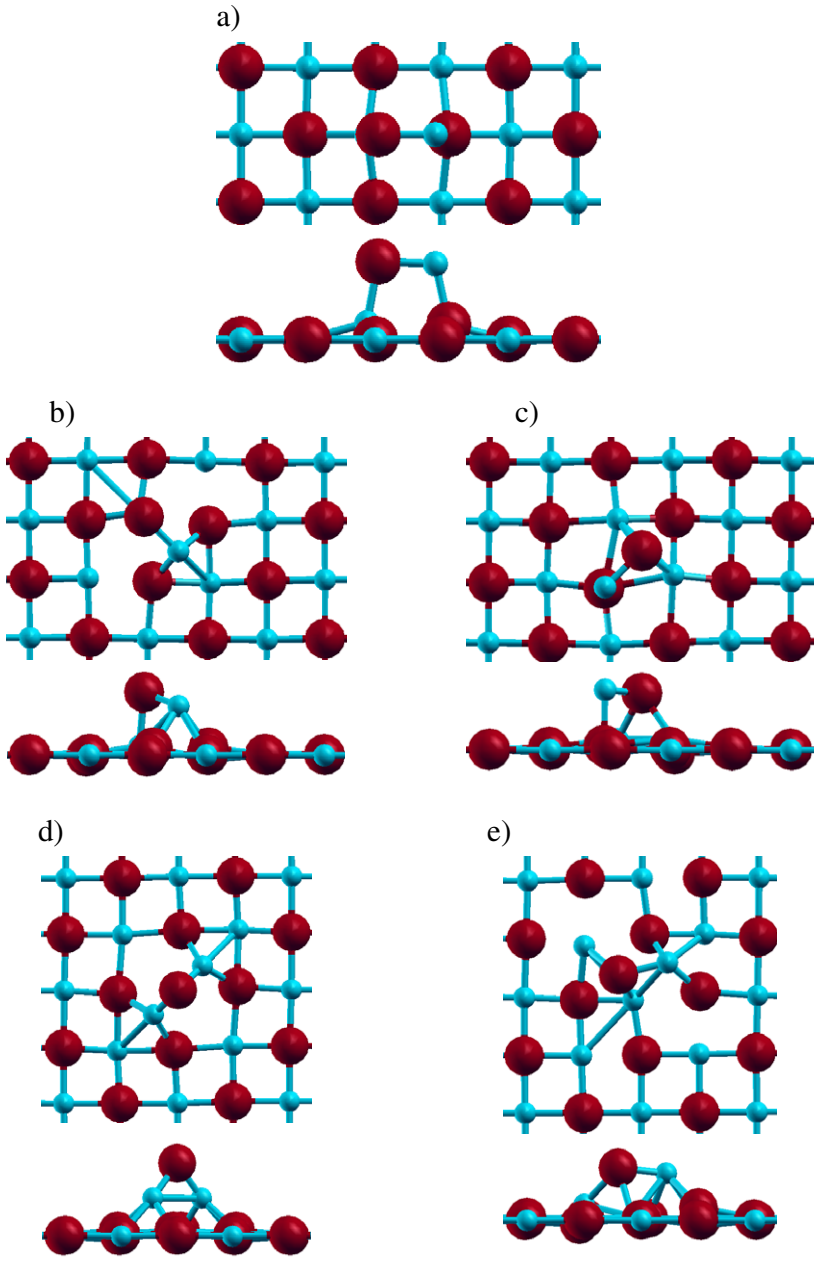

Figure 1. Top and side views of atomic configurations at $T = 0$ K. Mg ions, small spheres; O ions, large spheres. The interatomic bonds are guides for the eye. (a) Adsorbed MgO molecule on the (001) surface in its stable position. Intermediate states for (b) the Mg rotation, (c) the O rotation, (d) the Mg exchange and (e) the MgO molecular jump mechanisms.

enthalpy is not successfully reproduced. The molecule adsorption enthalpy is better reproduced by the Matsui potential whereas the cluster formation enthalpies are better reproduced by the Okada one.

We finally choose the Matsui potential because it is the one that generally agrees with all the *ab initio* data, especially for the cohesive energies and the bonding properties of the molecule on the flat surface.

3.2. Diffusion mechanisms

The molecule spends most of its time on regular lattice sites in stable positions (figure 1(a)). Four different mechanisms have been observed during the analysis of the trajectories of a MgO molecule diffusing on the flat surface. (i) Mg rotation: the admolecule pivots 90° around its O ion with the intermediate configuration at 45° with the molecular axis roughly parallel to the surface plane (figure 1(b)). (ii) O rotation: the molecule pivots 90° around its Mg ion with the intermediate configuration at 45° with the molecular axis roughly parallel to the surface plane (figure 1(c)). (iii) Exchange of Mg: Mg turns around O, reaching the configuration of the Mg rotation, and pushes the Mg ion below O from the surface plane. Then, the Mg adatom replaces the Mg (below) which binds to the O adatom (figure 1(d)). (iv) The simultaneous jump of both ions towards new sites, referred to hereafter as a 'molecular jump' (figure 1(e)).

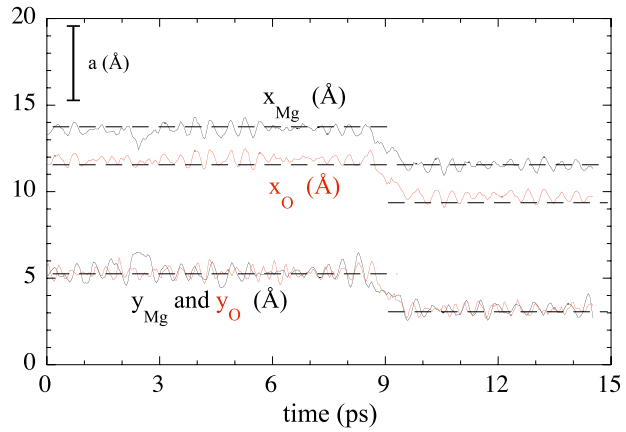

Figure 2. MgO molecular jump mechanism. An example of a MD trajectory ($T = 706$ K) in which the atomic coordinates are plotted as a function of the time. When this jump occurs, the two in-plane Cartesian coordinates of Mg and O undergo simultaneously a variation of $a/2$ (a is the lattice parameter).

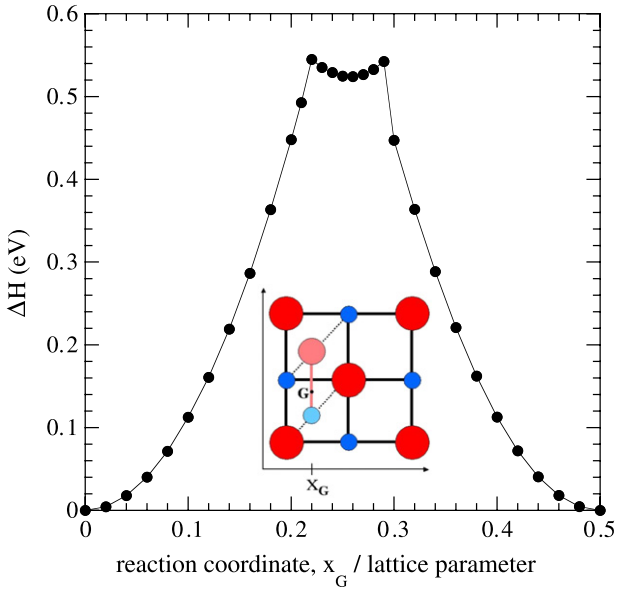

Figure 3. MgO molecular jump enthalpy profile as a function of the reaction coordinate. The reaction coordinate x_G is one of the coordinates of the centre of mass of the migrating molecule. A schematic view of the diffusion path is given in the inset.

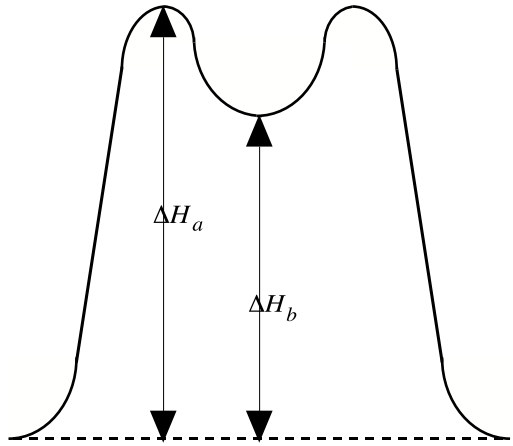

Figure 4. Schematic definitions of the enthalpies ΔH_a and ΔH_b associated with the jumps. ΔH_a represents the activation enthalpy whereas ΔH_b is the enthalpy difference between the intermediate configuration and the initial one.

The three first mechanisms have already been observed, whereas the molecular jump is a new diffusion process. It is not the combination of an O rotation and an Mg rotation as shown by figure 2. In fact, the in-plane atomic coordinates of the molecule change simultaneously by $a/2$ and not consecutively. We have focused on this novel mechanism by calculating the static energy profile as a function of the associated reaction coordinate. It is defined by the x-coordinate of the centre of mass of the molecule. This was achieved by performing DFT-GGA (see section 2.1) calculations under constraint. This profile given in figure 3 displays an intermediate state 0.02 eV lower than the top of the energy barrier, 0.54 eV.

At low temperature (700–900 K), the main mechanism is the Mg rotation followed by the exchange one, as shown in table 2. At high temperature (900–1100 K) the exchange mechanism becomes dominant. This change comes from the variation from 0.26 to 0.12 eV of the activation enthalpy (see table 2) of the Mg exchange occurring at 900 K. Whatever the temperature, the two other types of mechanism (O rotation and molecular jump) represent less than 2% of the jumps. This can also be noted by comparing the activation enthalpies: the same value of 0.50 eV for the two jumps involving O adatoms (O rotation or molecular jump) and less than 0.26 eV for Mg jumps (rotation or exchange). At 900 K, the time of flight associated with the Mg exchange is approximately twice the values corresponding to the other mechanisms. Indeed, we observed that the adatoms remain for a long time in an intermediate state consisting of a triangular configuration described in figure 1(d).

Except in the case of the molecular jump, the mechanisms do not produce transport of matter as they are considered alone. It is the combination of all the mechanisms that leads to diffusion. The corresponding diffusion coefficient is unique and cannot characterize each mechanism independently. Since a single molecule migrating on a surface would require trajectories that are too long to obtain directly an accurate enough diffusion coefficient (which is not the case for the jump frequencies), we were not able to compute this quantity.

3.3. Activation energies

The enthalpies ΔH_a correspond to the height of the barrier when the system leaves the initial stable configuration and represent the true activation energies. On the contrary, the enthalpies ΔH_b refer to an intermediate state that is not the highest energy configuration but a local energy minimum midway between the initial and final configurations (figure 4). They are not relevant for characterizing the jump frequencies. These quantities are used to compare the Matsui and DFT-GGA approaches (figure 5), both calculated in the same conditions.

The static values of ΔH_a have been computed with the Matsui potential in the case of Mg and O rotations. This was achieved by a constraint optimization procedure similar to

Table 2. MgO diffusion mechanisms. Contributions of each jump observed in the MD simulation based on the Matsui empirical potential together with associated activation enthalpies, ΔH_a. The dynamical results refer to Arrhenius plots of the jump frequencies performed in the temperature range [700, 1100 K]. The corresponding times of flight, τ, are given at 900 K. Static calculations are given both within DFT-GGA and with the Matsui potential. ΔH_b represents the enthalpy difference between the intermediate configuration and the initial one.

	Dynamical calculations—Matsui potential					Static calculations		
	% of jumps[a]		ΔH_a (eV)		τ (ps)	Matsui	Matsui	GGA
Mechanism	700 K	1000 K	700–900 K	900–1100 K	900 K	ΔH_a (eV)	ΔH_b (eV)	ΔH_b (eV)
Mg rotation	70.9	27.3	0.20 ± 0.01	0.20 ± 0.01	1.07 ± 0.07	0.26	0.17	0.35
O rotation	0.6	0.8	0.50 ± 0.05	0.50 ± 0.05	0.8 ± 0.3	0.61	0.61	0.46
Mg exchange	26.2	69.0	0.26 ± 0.02[b]	0.12 ± 0.02[b]	1.76 ± 0.07		0.21	0.28
Molecular jump	0.6	0.8	0.50 ± 0.05	0.50 ± 0.05	1.07 ± 0.15		0.48	0.54

[a] The sum does not equal unity because mixed mechanisms are not reported.
[b] The effective value in the temperature range [700, 1100 K] is 0.20 ± 0.02 eV.

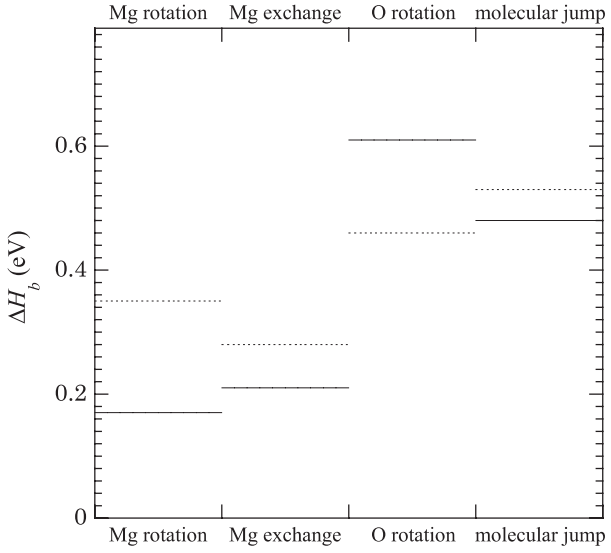

Figure 5. Enthalpy difference between the intermediate and initial configurations of the jumps, ΔH_b. Matsui potential, full line; DFT-GGA, dotted line.

that described in [10] (damped molecular dynamics and fixed distance constraint), the reaction coordinate being the distance between the rotating atom and the surface atom onto which it finally adsorbs. The Matsui static activation enthalpies (see table 2) are higher than the dynamical ones. The dynamical approach is therefore useful so as not to overestimate the energy barriers.

The discrepancy between the Matsui and DFT-GGA approaches (table 2) varies as a function of the actual mechanism. It is quite large for Mg (−51%) and O (+33%) rotations whereas it is smaller for the Mg exchange (−25%) and the molecular jump (−9%). Since we consider the DFT-GGA values as the reference, the Matsui potential underestimates the energy of the intermediate state in the cases of Mg rotation and exchange whereas it dramatically overestimates that of the O rotation. However, the two approaches provide the same picture: the two mechanisms only involving the Mg adatom are very frequent while the two mechanisms involving the O adatom are more unlike. The O adatom jump is obviously the limiting step for admolecule diffusion.

All the results are in good agreement with the complementary investigations of Harris *et al* [12] and Henkelman *et al* [11]. For instance, their description of the elementary mechanisms presenting an intermediate local minimum is in good agreement with our results. Henkelman *et al* found no intermediate minimum for the O rotation mechanism. This is corroborated by the equality of the values of ΔH_a and ΔH_b given in table 2. The ΔH_b values calculated by these authors in the GGA-PW91 formalism are 0.31 eV for Mg rotation, 0.43 eV for O rotation and 0.24 eV for Mg exchange, to be compared with our values of 0.35, 0.46 and 0.28 eV, respectively, in the GGA-PBE formalism. Interestingly, the cation exchange mechanism was suggested by Harris *et al* to be at the root of interdiffusion at the interface between two oxides.

3.4. Implications for crystal growth and comparison with surface diffusion in metals

Whatever the deposited species, atoms or molecules, we have already shown [10] that the most stable and the most mobile entity is the MgO molecule, which plays a crucial role in the growth. After its deposition or its formation, the admolecule can move easily on the flat surface. This diffusion must be taken into account in any relevant modelling of the growth. The two fastest mechanisms, Mg rotation and exchange, do not allow the migration of the molecule since the oxygen atom remains fixed. The two complementary mechanisms, O rotation and molecular jump, although much less frequent, allow the oxygen adatom to leave its regular site and are therefore necessary to yield the long-range displacement of the molecule.

The static energy barrier associated with the O exchange calculated by Henkelman *et al* is 0.88 eV, which indicates that such a mechanism is rather dissimilar. Indeed, we did not observe such a migration with the Matsui potential. Nevertheless, occurrences of O exchange were seen in additional MD computations based upon the Okada potential. However, in these simulations O rotation was not observed.

Interestingly, the surface diffusion of metal atoms on metallic surfaces, which has been studied for a long time, implies atomic jumps including exchange mechanisms. Widely studied on fcc(110) and fcc or bcc(001) surfaces, these exchange mechanisms usually involve much higher energy

barriers (in the range 0.6–0.9 eV) [1] than the small barrier found in the present study (effective barrier of 0.20 eV).

4. Summary and conclusions

In this paper, we have presented a systematic study of the diffusion mechanisms of a MgO admolecule on the MgO(001) flat surface. Four mechanisms have been identified and their dynamical and static barriers calculated. Among these mechanisms, one (molecular jump) had not been reported yet to our knowledge. An interesting Mg exchange mechanism, already predicted, has been found to be very frequent and has a very low activation energy. This mechanism competes with pure Mg rotation. However, the two other mechanisms, that are not so frequent and involve a displacement of the oxygen adion, are necessary to produce long-range diffusion of the MgO admolecule. These results are currently being used as input into kinetic Monte Carlo simulations of the crystal growth of the magnesium oxide.

Such investigations about the microscopic mechanisms complete experimental observations on MgO(001) surfaces [22–28]. In fact, the diffusion of a MgO admolecule on the MgO surface has not been studied experimentally. This should not be too surprising, since a phenomenon concerning a single molecule is difficult to investigate. The most relevant experimental work on MgO surfaces (without admolecule) has been done by scanning force microscopy [22] and mostly concerns the deposition of metallic clusters. Scanning tunnelling microscopy experiments made on MgO ultrathin films deposited on metallic electrodes [23, 24] allow one to gain an insight into the shape and direction of steps.

Acknowledgments

Figure 1 has been drawn with the XCRYSDEN software [29]. Some of these calculations were performed on the CNRS-IDRIS supercomputers.

References

[1] Antczak G and Ehrlich G 2007 *Surf. Sci. Rep.* **62** 39
[2] Itoh M 2001 *Prog. Surf. Sci.* **66** 53
[3] Freitas P P, Ferreira R, Cardoso S and Cardoso F 2007 *J. Phys.: Condens. Matter* **19** 165221
[4] Kantorovich L N and Gillan M J 1997 *Surf. Sci.* **374** 373
[5] Geneste G, Morillo J and Finocchi F 2002 *Appl. Surf. Sci.* **188** 122
[6] Geneste G, Morillo J and Finocchi F 2003 *Surf. Sci.* **532–535** 508
[7] Finocchi F, Geneste G, Morillo J and Hayoun M 2003 *Crystal Growth: From Basic to Applied* ed S Carra and C Paorici (Roma: Accademia Nazionale dei Lincei) p 121
[8] Geneste G, Morillo J, Finocchi F and Hayoun M 2004 *Materials Research Society Fall Mtg 2003 (Boston)*; *Mater. Res. Soc. Proc.* **786** 365
[9] Geneste G, Morillo J and Finocchi F 2005 *J. Chem. Phys.* **122** 174707
[10] Geneste G, Morillo J, Finocchi F and Hayoun M 2007 *Surf. Sci.* **601** 5616
[11] Henkelman G, Uberuaga B P, Harris D J, Harding J H and Allan N L 2005 *Phys. Rev.* B **72** 115437
[12] Harris D J, Lavrentiev M Y, Harding J H, Allan N L and Purton J A 2004 *J. Phys.: Condens. Matter* **16** L187
[13] Kohn W and Sham L J 1965 *Phys. Rev.* **140** A1133
[14] Gonze X, Beuken J M, Caracas R, Detraux F, Fuchs M, Rignanese G M, Sindic L, Verstraete M, Zerah G, Jollet F, Torrent M, Roy A, Mikami M, Ghosez P, Raty J Y and Allan D C 2002 *Comput. Mater. Sci.* **25** 478
[15] Perdew J P, Burke K and Ernzerhof M 1996 *Phys. Rev. Lett.* **77** 3865
[16] Bader R W 1991 *Chem. Rev.* **91** 893
[17] Allen M P and Tildesley D J 1987 *Computer Simulation of Liquids* (Oxford: Clarendon) p 156
[18] Kubo M, Oumi Y, Miura R, Fahmi A and Stirling A 1997 *J. Chem. Phys.* **107** 4416
[19] Shen Q and Ellis D E 1995 *Phys. Rev.* B **51** 15732
[20] Okada I, Utsunomiya Y, Uchida H and Aizawa M 2002 *J. Mol. Liq.* **98/99** 191
[21] Matsui M 1989 *J. Chem. Phys.* **91** 489
[22] Barth C and Henry C R 2003 *Phys. Rev. Lett.* **91** 196102
[23] Gallagher M C, Fyfield M S, Bumm L A, Cowin J P and Joyce S A 2003 *Thin Solid Films* **445** 90
[24] Schneider W D 2002 *Surf. Sci.* **514** 74
[25] Peterka D, Tegenkamp C, Schröder K M, Ernst W and Pfnür H 1999 *Surf. Sci.* **431** 146
[26] Wollschläger J, Viernow J, Tegenkamp C, Erdös D, Schröder K M and Pfnür H 1999 *Appl. Surf. Sci.* **142** 129
[27] Vassent J L, Marty A, Gilles B and Chatillon C 2000 *J. Cryst. Growth* **219** 434
[28] Vassent J L, Marty A, Gilles B and Chatillon C 2000 *J. Cryst. Growth* **219** 444
[29] Kokalj A 2003 *Comput. Mater. Sci.* **28** 155 Code available from http://www.xcrysden.org/